JGR Atmospheres

RESEARCH ARTICLE
10.1029/2019JD032006

Key Points:
- Prominent environmental and structural differences exist between developing and nondeveloping circulations
- The major environmental factors impeding the development of an initial circulation to a tropical storm vary from basin to basin
- Nondeveloping cases have a weaker protective layer "shear sheath" around the vortex core at midlevels, leading to dry-air intrusion

Supporting Information:
- Supporting Information S1

Correspondence to:
P. H. Raavi,
praavi@student.unimelb.edu.au

Citation:
Raavi, P. H., & Walsh, K. J. E. (2020). Basinwise statistical analysis of factors limiting tropical storm formation from an initial tropical circulation. *Journal of Geophysical Research: Atmospheres*, *125*, e2019JD032006. https://doi.org/10.1029/2019JD032006

Received 11 NOV 2019
Accepted 22 APR 2020
Accepted article online 26 APR 2020

Basinwise Statistical Analysis of Factors Limiting Tropical Storm Formation From an Initial Tropical Circulation

Pavan Harika Raavi[1,2] **and K. J. E. Walsh**[1,2]

[1]School of Earth Sciences, University of Melbourne, Melbourne, Victoria, Australia, [2]ARC Centre of Excellence for Climate Extremes, University of New South Wales, Sydney, New South Wales, Australia

Abstract Tropical cyclones (TCs) form within a closed circulation region of large-scale disturbances under certain dynamical and thermodynamical conditions. This study investigates differences in the large-scale environmental conditions of a TC 48 hr before the declaration of tropical depression, comparing those that developed into tropical storms (TSs) with those depressions that did not develop. Here, we apply the Okubo-Weiss Zeta Parameter detection and tracking scheme to ERA-interim reanalysis from 1989–2018, across different ocean basins. The method detects storm-system-scale environmental conditions that favor TC formation. We construct spatial composites of thermodynamical and dynamical quantities for both developing and nondeveloping depressions, as well as storm-relative streamlines. A statistical index (the Box Difference Index) is used to quantitatively estimate the dominant limiting factors of TS formation from the area-averaged quantities of large-scale variables. The relative contribution of large-scale environmental variables impeding the development of an initial tropical depression to TS differs between ocean basins perhaps due to regional variations in the characteristics of large-scale disturbances and the surrounding environmental conditions. A streamline analysis shows that the developing storms have a more pronounced cyclonic core and are protected from external influences by a stronger shear sheath layer surrounding the core extending from the lower to middle troposphere. This study, therefore, identifies the potential limiting variables and structural differences in an initial circulation that impede TS formation across different ocean basins.

Plain Language Summary Tropical cyclones form under certain atmospheric conditions within different large-scale disturbances across various ocean basins. Every year a large number of tropical disturbances form across global ocean basins, but only a few of them develop into tropical cyclones, with a geographical variation in the number of formations. Previous studies on the differences in the environmental conditions of developing versus nondeveloping tropical disturbances focus on the Atlantic and Pacific Ocean basins due to less observations in other ocean basins. The recent development of the "marsupial pouch" theory of tropical cyclone formation has led to the development of a detection scheme to identify the locations within large-scale disturbances that have the potential for tropical cyclone formation. The detection scheme is tuned to detect the initial tropical depressions in addition to the developed tropical storms. This scheme helps us to investigate the environmental differences between developing and nondeveloping tropical depressions in all the ocean basins. The environmental variables inhibiting tropical storm formation differ among ocean basins, with structural differences from the lower to upper troposphere disrupting sustained convection in nondeveloping cases. This study, therefore, identifies the potential limiting factors for tropical storm formation across different ocean basins.

1. Introduction

Tropical cyclones (TCs) are highly destructive extreme events that lead to substantial socioeconomic losses, primarily in coastal regions. TCs form under certain favorable thermodynamical and dynamical conditions within closed recirculating regions (Dunkerton et al., 2009; Gray, 1968, 1975). Favorable thermodynamical conditions include sea surface temperatures higher than 26.5°C, a deep layer of a conditionally unstable environment, and moist midtroposphere (Gray, 1968). Dynamical conditions include weak to moderate vertical wind shear (vector wind difference magnitude between the 850 and 200 hPa), deep organized convection, and locally enhanced values of low-level cyclonic relative vorticity (Gray, 1968, 1975; McBride & Zehr, 1981). Additionally, Gray (1968) suggested that TCs generally do not form within 5° of the equator.

Although these conditions are necessary for TC formation, it is still not clear what are the sufficient conditions, due to multiscale interactions in the TC formation activity.

TC formation undergoes different stages of development. The first stage involves preconditioning of the large-scale environment along with the formation of minimum atmospheric pressure in the lower levels. The second stage involves the formation of a self-sustaining mesoscale vortex and its aggregation, with modest stretching and shearing deformations enabling a near-solid body rotation (Briegel & Frank, 1997; Dunkerton et al., 2009; Lee et al., 1989; Montgomery et al., 2006; Ritchie & Holland, 1999). Some large-scale disturbances provide suitable conditions such as increasing low-level relative vorticity, convective activity associated with increased updraft strength, and altering the vertical wind shear distribution to conditions favorable for TC formation. These disturbances include (1) tropical depression (TD)-type waves, also called African easterly waves (AEWs) in the North Atlantic (NA) region (Landsea, 1993; Thorncroft & Hodges, 2001); (2) Rossby wave trains induced by a preexisting TC, Pacific easterly waves and synoptic wave trains, or TD-type waves in the western North Pacific (WNP) region (Fu et al., 2007; Li et al., 2006; Li & Fu, 2006; Xu et al., 2013); and (3) equatorial Rossby waves and mixed Rossby-gravity waves in the South Indian Ocean (SI), South Pacific (SP), and Australian (AUS) regions (Bessafi & Wheeler, 2006; Frank & Roundy, 2006; Hall et al., 2001). Other forms of large-scale disturbances favorable for TC formation are the monsoon trough, regions with upper-level troughs and low-level wind surges (Briegel & Frank, 1997; Ferreira & Schubert, 1997; Ritchie & Holland, 1999; Wang & Magnusdottir, 2005, 2006; Zong & Wu, 2015).

Every year a large number of TDs form in global ocean basins from various types of tropical disturbances. However, despite apparently suitable conditions provided by these disturbances, not all the depressions develop into tropical storms (TSs). For instance, in the NA, a large number of AEWs form every year, but only around 30% of them develop into TSs (Avila, 1991). Understanding of the TC formation pathway has recently been advanced by the "marsupial paradigm" defined within tropical easterly waves over the Atlantic and Pacific regions (Dunkerton et al., 2009). This innovative work recognizes that TCs form in a relatively rare recirculating region called a pouch within a critical layer of the tropical wave under favorable surrounding conditions. A deep pouch from the low to middle troposphere within an easterly wave maintains an area of closed circulation, where the entry of outside air is restricted, shelters the storm from disruptive influences, and enables it to intensify under a favorable environment (Montgomery et al., 2010; Wang et al., 2010a, 2010b, 2012).

Asaadi et al. (2016, 2017) found that developing easterly waves appear to propagate as a packet of four to five waves, tilted somewhat northwest-southeast from zonal. Also, of these waves, only one wave is located at the critical latitude (where the mean flow speed equals phase speed of the wave) and in a region of weak potential vorticity gradient, where TC formation can occur. These studies highlighted the role of a deep pouch and the critical latitudes of the easterly waves favorable for TC formation.

Peng et al. (2012) and Fu et al. (2012) examined the environmental differences between developing and nondeveloping tropical disturbances detected by time filtering technique to extract synoptic-scale disturbances (tropical waves). They noted that thermodynamical conditions are more important across the NA basin, and dynamical conditions are more critical across the WNP basin. These studies showed that the relative contribution of large-scale variables to TC formation varies between these two basins due to distinctive large-scale disturbances and varying regional environmental conditions. It is, therefore, essential to study differences between developing and nondeveloping cases across global ocean basins that have diverse environmental conditions and distinct large-scale disturbances to identify the important predictors for TC formation.

There are many other studies on the environmental differences between the developing and nondeveloping AEWs across the NA basin (Brammer & Thorncroft, 2015; Davis & Ahijevych, 2012; Fowler & Galarneau, 2017; Hopsch et al., 2010; Komaromi, 2013; Montgomery & Smith, 2010). These studies highlight the importance of relative flow within AEWs, increased low-level vorticity, vertical shear, and sufficient tropospheric moisture for the development of an initial disturbance. A moist midtroposphere increases the strength of convective updrafts by decreasing the effect of dry air, which disrupts the deep convection (Nolan, 2007; Smith & Montgomery, 2012; Z. Wang, 2012). Persistent broad-scale, deep convection can then spin up the primary vortex via a system-scale convergence by the in-up-out secondary circulation (Hendricks et al., 2004; Montgomery et al., 2006; Raymond & Sessions, 2007; Tory et al., 2007; Tory, Montgomery & Davidson, 2006; Tory, Montgomery, Davidson & Kepert, 2006).

Some studies found that moderate shear or easterly shear is favorable for developing cases (Tuleya & Kurihara, 1981, 1982; Zehr, 1992; Zeng et al., 2010). In contrast, enhanced vertical wind shear misaligns the storm, which sometimes leads to ventilation, thereby disrupting the intensification process (Alland et al., 2017; Davis & Ahijevych, 2012; Riemer et al., 2010; Tang & Emanuel, 2010; Wang et al., 2012). Other studies showed that abundant low-level convergence and enhanced mass flux through organized outflow is associated with sustained deep convection in developing cases, with an anticyclonic circulation in the upper levels (Lee, 1989a, 1989b; McBride & Zehr, 1981; Sears & Velden, 2014; Tuleya, 1991; Zehr, 1992; Zhang & Zhu, 2012).

In addition to the above studies on environmental differences, from particle trajectory analysis around the developing storms in the NA basin, Rutherford et al. (2015) identify a protective layer termed the "shear sheath" surrounding the core of the storm that can inhibit shear-induced storm weakening. This shear sheath is a layer of high deformation (i.e., a strain-dominated region) that serves to isolate the core from its surroundings. These strain-dominated regions are termed as the rapid filamentation zones, where convection is suppressed, and subsidence is more pronounced (Rozoff et al., 2006). The shear sheath acts as a barrier layer that protects the initial vortex from external influences by obstructing the horizontal inflow of dry air or opposite signed vorticity fields into the core region of developing storms. Rutherford et al. (2015, 2018) found that the development of a TD to a TS involves a notable shear sheath region around the vortex core region.

From the studies above, we note that there are no global studies on the environmental and structural differences between the developing and nondeveloping circulations. In the current study, we use a phenomenon-based TC detection and tracking scheme to detect the initial circulations and identify the environmental and structural differences across different ocean basins. This TC detection scheme is developed based on the marsupial paradigm of TC formation. It detects the low deformation vorticity regions within the pouch that have the potential for TS formation by using a diagnostic (OWZ) along with other environmental variables. This diagnostic is a product of the normalized Okubo-Weiss (OW) parameter and absolute vorticity (Zeta) parameter (Tory, Chand, Dare, & McBride, 2013, Tory, Chand, McBride, et al., 2013; see section 2 for a more detailed description). The Okubo-Weiss Zeta Parameter (OWZP) tracking scheme detects both a TS, that is any TC with low-level winds higher than 17 m/s, and a TD, that is any TC weaker than a TS. We consider those TDs that become TSs as developing TCs and the remaining TDs nondevelopers (Tory et al., 2018). This tracking scheme is particularly helpful in the basins where there are no observational aircraft missions for identifying and tracking the initial depressions. Therefore, we perform a basinwide composite analysis on ERA-Interim reanalysis data using these detected circulations to identify the limiting factors for the development of an initial TD.

From the above literature, TC formation from an initial circulation requires a favorable "external environment," such as enhanced vorticity, low-level cyclonic circulation, a moist atmospheric column, and weak to moderate vertical wind shear. As the circulation intensifies, the "internal environment" (the core of the circulation) becomes more favorable: it becomes moister, vorticity amplifies, and the shear sheath layer around the core strengthens. It is, therefore, difficult to separate the internal and external environment, so a more developed TC looks like it is in a more favorable environment than a weaker TC. By focusing on the differences between developing and nondeveloping TCs 48 hr before the TD declaration, we have some confidence that most of the differences we identify are likely to be external rather than internal. This composite analysis helps us to find out the external environmental conditions and structural variations that assist or hinder TS formation, and whether these conditions are similar or differ between ocean basins.

Section 2 of the paper describes the data and methods. Sections 3 and 4 provide the results and discussion, respectively, while section 5 summarizes the conclusions.

2. Data and Methodology

2.1. TS Observations and ERA-Interim Data

The observed TS information from 1989 to 2018 is from the International Best Track Archive for Climate Stewardship (IBTrACS) database (Knapp et al., 2010). The TS genesis location of IBTrACS is the first position at which the system satisfies a maximum sustained low-level 10-min wind speed higher than 33

knots (17 m/s) during its lifetime. The reanalysis fields are taken from the ERA-Interim data, compiled by the European Centre for Medium-Range Weather Forecasts (Compo et al., 2011; Dee et al., 2011). These data have a horizontal resolution of 0.75 ° × 0.75°. We extract the data for a period of 30 years, from 1989 to 2018, at 12-hourly intervals (00 and 12 UTC) to create variables used by (i) the TC detector and (ii) the composite analysis of the environmental conditions.

The variables used by the detector at 12-hourly intervals (00 and 12 UTC) include the zonal (u) and meridional (v) wind fields, to compute (1) the OWZ at both 850- and 500-hPa pressure levels (Tory, Chand, McBride, et al., 2013); (2) vertical wind shear (vector wind difference magnitude) between 850- and 200-hPa pressure levels; and (3) the TC steering velocity (the average wind at 700 hPa within a 4 ° × 4° box region around the grid point center) (Tory, Dare, Davidson, et al., 2013). Additional parameters include relative humidity (RH) at 700 and 500 hPa and 950-hPa specific humidity (SH_{950}).

The OW parameter is a relative measure of vorticity to deformation forces that identifies the rotation dominant regions, along with strain dominated areas such as the shear sheath:

$$OW = \zeta^2 - \left(E^2 + F^2\right) \tag{1}$$

where $\zeta = \left[\frac{\partial v}{\partial x}\right] - \left[\frac{\partial u}{\partial y}\right]; E = \left[\frac{\partial u}{\partial x}\right] - \left[\frac{\partial v}{\partial y}\right]; F = \left[\frac{\partial v}{\partial x}\right] + \left[\frac{\partial u}{\partial y}\right]$

Here, ζ is the relative vorticity, and E and F represent the stretching and shearing deformation respectively.

Tory, Dare, Davidson, et al. (2013) and Tory, Chand, Dare, and McBride (2013) show that the enhanced values of OWZ identify the system-scale low-deformation vorticity regions of solid body rotation. Therefore, the phenomenon-based TC detection and tracking scheme (OWZP) uses the diagnostic variable OWZ, which replaces the absolute vorticity variable of other traditional TC tracking schemes. The OWZ calculation involves normalization of the OW parameter by the square of the relative vorticity. The OWZ uses only positive values which include a range of flows, from deformation-dominated flows ($OW_{norm} = 0$) to rotation dominant regions ($OW_{norm} = 1$). The phenomenon-based TC tracking scheme uses the thresholds of the OWZ variable instead of the OW variable.

The equation representing the OWZ is

$$OWZ = \max(OW_{norm}, 0) \times (\zeta + f) \times sign(f) \tag{2}$$

$$OW_{norm} = \frac{OW}{\zeta^2} \tag{3}$$

Here OW_{norm} is the normalized OW parameter, and f is the Coriolis parameter.

The variables used to examine the composite storm environment are those already found to be important for TC formation (Camargo et al., 2007; Ditchek et al., 2017; Emanuel & Nolan, 2004; Gray, 1968; McBride & Zehr, 1981; Tippett et al., 2011; Tory, Chand, McBride, et al., 2013). These variables include the total column water (TCW; in units of kg/m^2), 700-hPa RH (%), maximum potential intensity (MPI; m/s), 850-hPa Relative vorticity (*RVor;* $s^{-1} \times 10^{-6}$), 500-hPa Omega (Omega; Pa/s), 200-hPa divergence (DIV*;* $s^{-1} \times 10^{-6}$), vertical shear of zonal wind ($U_{200} - U_{850}$) (Ushear; m/s), and OW parameter ($s^{-2} \times 10^{-10}$). We consider the positive values of Ushear as westerly shear and negative values as easterly shear. Here, the signs of Omega globally and RVor in the Southern Hemisphere (SH) are reversed, meaning that positive Omega is now upward motion, and positive RVor in the SH is now cyclonic flow. We calculate the MPI using the equation formulated by Bister and Emanuel (1998):

$$MPI = \frac{T_s C_k}{T_o C_D}[CAPE_e - CAPE_b] \tag{4}$$

where T_s is the sea surface temperature, T_o is the outflow temperature, C_k denotes the enthalpy exchange coefficient, C_D denotes the drag coefficient, and *CAPE* is the convectively available potential energy with the subscripts e and b denoting the environmental and boundary layer atmospheric sounding respectively.

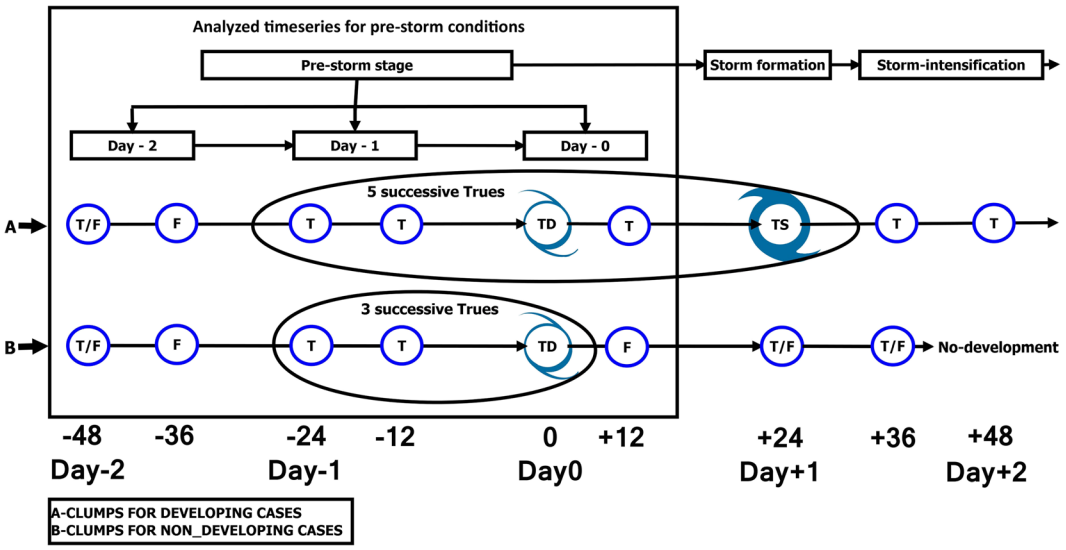

Figure 1. Diagram showing the tracks of developing and nondeveloping tropical depressions with F (False) indicating that the core thresholds are not satisfied and T (True) where the thresholds are satisfied. The third consecutive true is the TD declaration time for both developing and nondeveloping TDs. Path A shows that all TSs were once TDs, and Path B is a TD that did not develop into TS.

In addition to the above large-scale environmental variables, we use a meridional gradient of absolute vorticity (Beta*) variable:

$$\text{Beta}^{*} = \frac{\partial \eta}{\partial x} = \frac{\partial f}{\partial y} + \frac{\partial \zeta}{\partial y} \tag{5}$$

where η denotes the absolute vorticity. Tory et al. (2018) found that TC formation is favored in regions with lower values of the Beta* and is extremely rare in regions of enhanced values.

2.2. TC Detection and Tracking

Tory, Dare, Davidson, et al. (2013) found that 95% of observed TSs (IBTrACS) have enhanced values of OWZ at both 850- and 500-hPa levels relative to their surroundings, prompting them to base their OWZP TC tracking scheme on these two quantities along with other variables. The other atmospheric variables are RH at 700 and 950 hPa, SH at 950 hPa, and vertical wind shear. This scheme is designed to be applied to data on a $1^\circ \times 1^\circ$ grid. Therefore, we interpolate the ERA-interim data in the current study to $1^\circ \times 1^\circ$ grid resolution. Tory, Chand, McBride, et al. (2013) and Tory, Chand, Dare, & McBride (2013) give a detailed explanation of the detection scheme, which is a multistep process:

1. *Detect storms*: Identify circulations that have the potential for TC formation by testing every grid point with an initial set of threshold conditions (Table S1 in the supporting information of the supporting information gives the "initial" thresholds). Neighboring grid points satisfying the initial thresholds are clustered into individual clumps that represent the storm at specific times.
2. *Create storm tracks*: Individual storm tracks are constructed by linking the above instantaneous clumps forward in time based on the circulation's expected position from the 700-hPa steering flow, calculated as described in section 2.1. The tracks cease when there is no future circulation in the vicinity of the expected storm position.
3. *Detect TCs*: Figure 1 gives a schematic diagram of this process. At each point along the storm track, clump averages of different large-scale variables are assigned to each clump (storm) position. The core thresholds of Table S1 are checked with each clump position and labeled as "True" if the clump satisfies these core thresholds or "False" if not. Each storm track is assessed to see if it satisfies TD status, and then TS status. A particular track is declared a TS (TD) if it satisfies the core thresholds for at least 48 (24) hr consecutively, which amounts to five (three) consecutive true values for 12-hourly data.

Application of the TD and TS detection routine to 30 years of ERA-Interim data yielded 2,300 TSs and 3,432 TDs. The TD numbers include the 2,300 TSs, as all TSs were once TDs. This shows that the TD to TS ratio is about 3:2, implying globally there are 50% more lows that satisfy the TD than the TS thresholds, which is consistent with the 1979–2013 period considered by Tory et al. (2018). To obtain the nondeveloping depressions, we subtract the developed depressions (TSs) from the total TD data set. A total of 1,132 nondeveloping storms is detected, located across all the ocean basins. The fifth True position along the track of the TS (Figure 1) is considered as the TS genesis, which matches with the IBTrACS genesis position in most of the ocean basins (Bell et al., 2018) whereas third true position is considered as the TD genesis. Tory et al. (2018) tuned the OWZP scheme to detect the TDs in the tropical disturbance data set across the Australian region. Also, Bell et al. (2018) assessed the pregenesis tracks of the OWZP and IBTrACS TSs and noted that OWZP detected TSs have earlier tracks with longer duration because the scheme detects the locations that have potential for TS formation rather than the matured TSs.

2.3. Storm-Centered Spatial Composites of Developing and Nondeveloping Cases

To understand the environmental differences between developing and nondeveloping TDs, storm-centered composites of the environmental variables are created within a 24° × 24° region around the depression center. Also, we calculated the streamlines of the composite storm overlaid with the OW parameter and RH contours to understand the structural differences and the influence of the surrounding environment on the initial circulation. We include only the storms with a detected storm track that existed 48 hr before TD declaration. This group contains developing (PDV48) and nondeveloping storms (PND48) across each ocean basin (Table S2 shows basin boundaries). The analysis considers three periods: 48 and 24 hr before the time of TD formation, and the day of TD declaration, labeled Day 2, Day 1, and Day 0, respectively, as shown in Figure 1.

2.4. Statistical Index

To quantify the differences in the environmental conditions between the developing and nondeveloping TDs, we calculate the Box Difference Index (BDI) (Peng et al., 2012) for PDV48 and PND48 cases across all the ocean basins within a 12° × 12° box region around the depression center (blue boxes in Figure S1 in the supporting information). This domain size appears to show the maximum differences between developing (DV) and nondeveloping (ND) compared to the 24° × 24° region, which covers a larger spatial extent and may disrupt the box averages. The OW variable, which includes the vorticity dominated and shear sheath regions, is divided into two variables. For this we use a 9° × 9° box region (green boxes in Figure S1), the "OW center" variable uses the centered box showing the low-deformation vorticity strength and the "OW surrounding" variable determines the strength of the shear sheath uses the remaining boxes. The BDI index is defined as

$$BDI = \frac{mean(DV) - mean(ND)}{std(DV) + std(ND)} \tag{6}$$

where *mean (DV)* and *mean (ND)* are the mean of the environmental variables for DV and ND cases and *std (DV)* and *std (ND)* are the standard deviation of the DV and ND environmental variables, respectively. The higher the magnitude of the BDI (which ranges from 0 to 1), the better the variable can differentiate the two cases. The sign of the BDI index tells us the environmental behavior of the variable. In general, positive values indicate that the quantity favors development. However, the opposite is true for quantities in which small values favor TC formation, such as Ushear, Beta* and OW surrounding variables. The negative values of Ushear, Beta* and OW surrounding variables indicates favorable shear, barotropic stability regions and stronger shear sheath regions respectively that support the TC formation. We use a two-sample t test to determine the statistical significance of the differences between DV and ND cases.

3. Results

This section describes the storm-centered composite analysis of initial circulations that exists two days before TD declaration to identify structural differences and key limiting variables across each ocean basin that lead to the nondevelopment of an initial circulation.

3.1. Geographical Distribution of TS and TD Genesis Locations

Figure S2 shows the geographical distribution of genesis locations of IBTrACS and OWZP detected DV and ND depressions using the ERA-interim reanalysis. The genesis dots of the IBTrACS and the OWZP detected TSs have similar geographical locations in most of the ocean basins. Tory, Chand, Dare, and McBride (2013) statistically tested the performance of this TC detection scheme when compared with the IBTrACS for 20 years from 1989–2008. They showed globally 78% of IBTrACS storms are correctly detected using this scheme with a 25% false alarm rate. Also, of all the ocean basins the NI basin has poor performance, perhaps due to the NI being a unique land-enclosed basin and misidentification of the monsoon lows as TCs. We perform a basin-wide analysis of the mean annual frequency bias of the OWZP detected storms and IBTrACS for the 30 years 1989–2018. Table S3 shows that the NA, ENP, and SP basins have underpredicted genesis compared to observations. These negative biases across the ENP, NA, and SP basins may be due to more short-lived and land influenced storms compared to the WNP and SI basins that have more long-lived storms over the open ocean waters, which are usually detected well by the OWZP scheme (Tory, Chand, Dare, & McBride, 2013).

3.2. Structural Differences Between Developing and Nondeveloping TDs

Typically, a TS has a developed vortex core region from low level to midlevel with cyclonic circulation along with anticyclonic outflow at upper levels associated with a secondary circulation (Dunkerton et al., 2009; McBride & Zehr, 1981; Z. Wang et al., 2012). Additionally, developing cases have a stronger shear sheath layer from the low to midtroposphere around the core of the storm. This shear sheath protects the vortex core region from external influences like the horizontal intrusions of drier air or lower values of opposite sign vorticity (Rutherford et al., 2015, 2018). Therefore, structural variations, along with spatial distribution of environmental variables, are explored in detail 48 hr before TD declaration using spatial composites within a $24° \times 24°$ box region around the depression center across all the ocean basins. This box region covers a larger spatial extent including the centered cyclonic circulation and the surrounding region which helps us to understand the influence of external environment on the circulation.

3.2.1. Northern Hemisphere (NH) Basins

We examine the spatial composites of the atmospheric variables evolving from Day 2 to Day 0 to differentiate the DV and ND cases across the NA basin. The differences in the spatial composites of RH between the DV and ND cases in Figure 2a illustrate that developing cases have higher moisture at the center and surrounding regions compared to the nondeveloping cases from lower (850 hPa) to midtroposphere (500 hPa). Also, the DV cases have fully enclosed streamlines around the center at 500 hPa shown in Figure 4, whereas in ND cases streamlines gradually diverge to the northwest of the center on Day 0 with dry air surrounding the core region in the northwest side. Figure 2b indicates that ND cases have unfavorable shear at the center and surrounding areas compared to the DV cases as it propagates from Day 2 to Day 0 (Figure 5a shows averaged values of Ushear). The negative values of Uhsear indicate that ND cases have either stronger westerly shear (positive values) or weaker easterly shear (lower negative values). Also, Figure 2c shows that DV cases have increasing values of DIV from Day 2 to Day 0 at the center and surrounding regions compared to the ND cases indicating the development of stronger outflow jet associated with sustained convection in the DV cases. Similarly, Figure 2d shows that DV cases have higher values of MPI at the center and surrounding regions compared to the ND cases, indicating greater thermodynamic instability in DV cases.

We further examine the spatial composites of the OW parameter overlaid with streamlines in the comoving frame of the composite storm for both PDV48 and PND48 cases over the NA basin at 850-, 700-, 500-, and 200-hPa levels. Figures 3 and 4 show that closed or nearly closed streamlines surround the cyclonic cores from low levels to midlevels of the atmosphere. Each cyclonic circulation has a core of positive OW (strain-free rotation) surrounded by a band of negative OW (higher lateral strain, indicating the shear sheath), which extends from the lower (850 hPa) to the middle troposphere (500 hPa). A general decrease in the size and strength of the cyclonic circulation with height is evident, culminating in stronger anticyclonic outflow streamlines to the east of the center at 200 hPa for developing cases (Figure 4). In order to understand quantitatively the strength of centered circulation and the surrounding shear sheath in the DV and ND cases we use box averages of the OW center and OW surrounding parameters (Tables S4 and S5) as described in section 2.4. The OW center values of nondeveloping cases show that the cyclonic circulation is

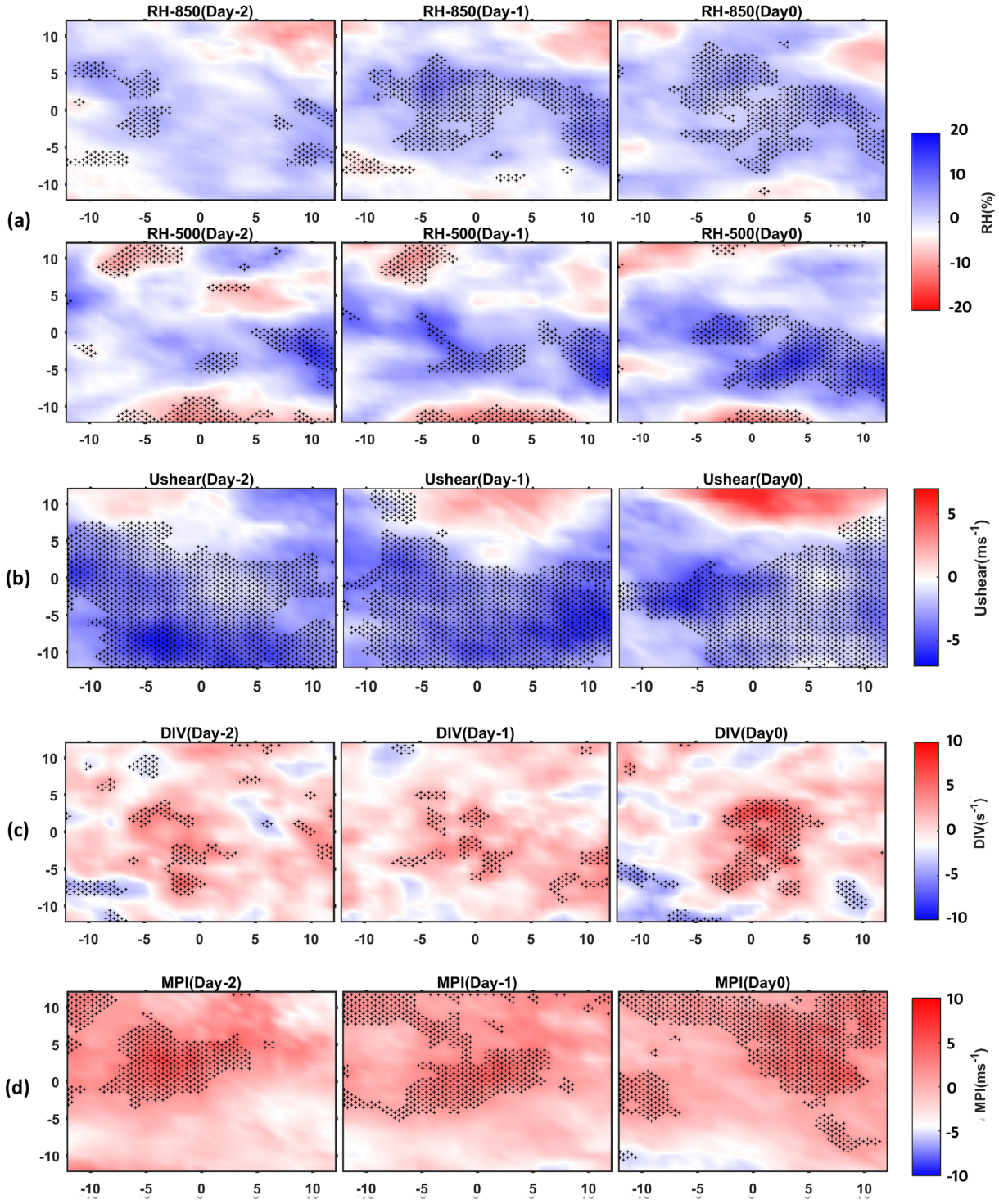

Figure 2. Differences in spatial composites of developing and nondeveloping cases (DV minus ND) within the 24 ° × 24° box region region around the circulation center over the North Atlantic basin, (a) 850 and 500 hPa RH, (b) Ushear, (c) DIV, and (d) MPI. The stippling indicates the 95% significance level differences.

significantly weaker than in the developing cases (Table S4). The OW surrounding values shows a development of a more pronounced shear sheath (higher negative OW values) in DV cases on Day 0 at both lower levels and midlevels (Table S5). The stronger the circulation, the stronger the OW core, and the stronger the shear sheath develops in DV cases.

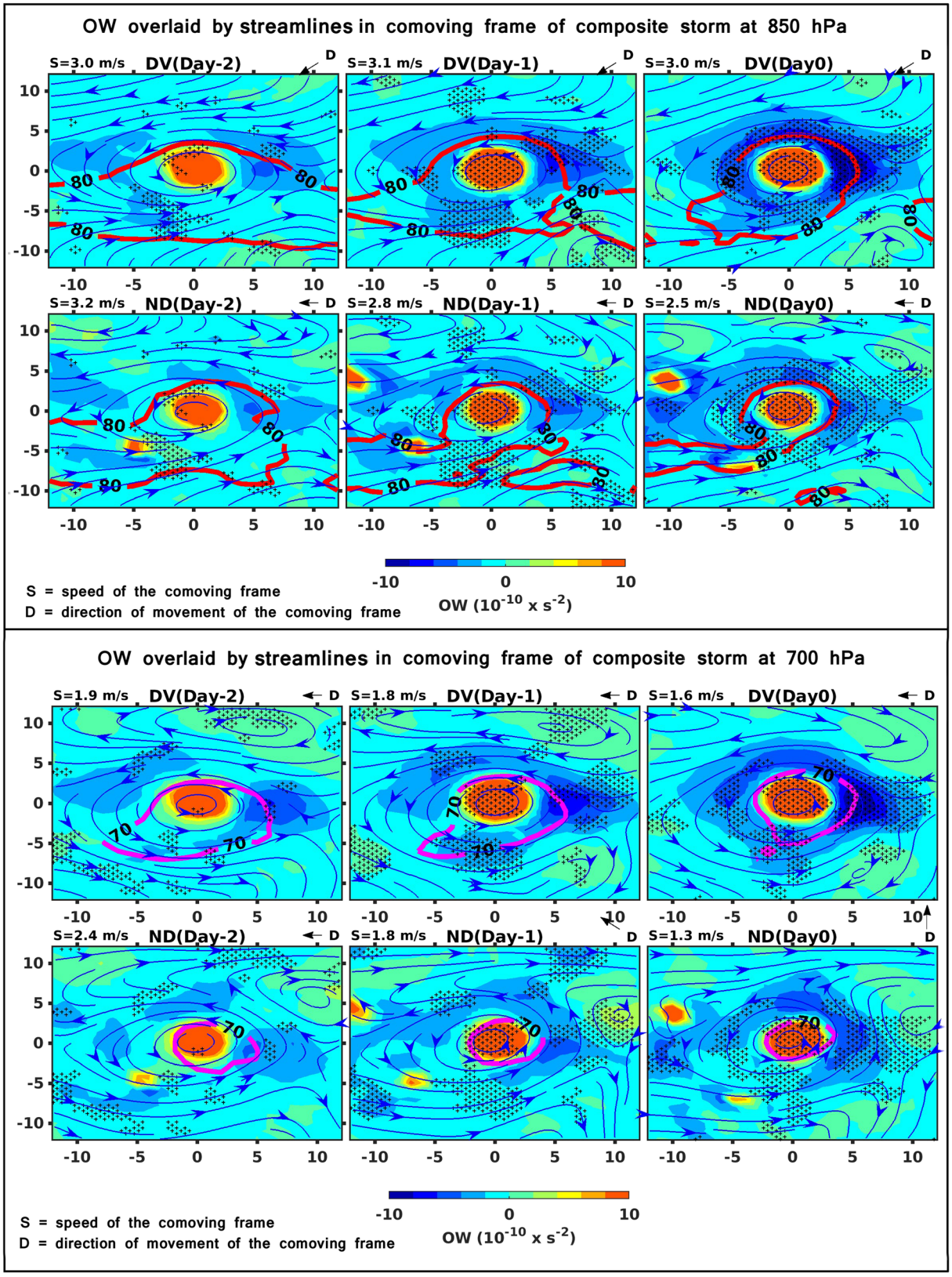

Figure 3. OW overlaid by streamlines computed in a comoving frame for DV and ND cases at 850 and 700 hPa over the North Atlantic basin. The *x* and *y* axes indicate the distance from the center in degrees, the red and magenta contours indicate 80% and 70% RH, respectively, and stippling indicates the 95% significance level differences between DV and ND cases.

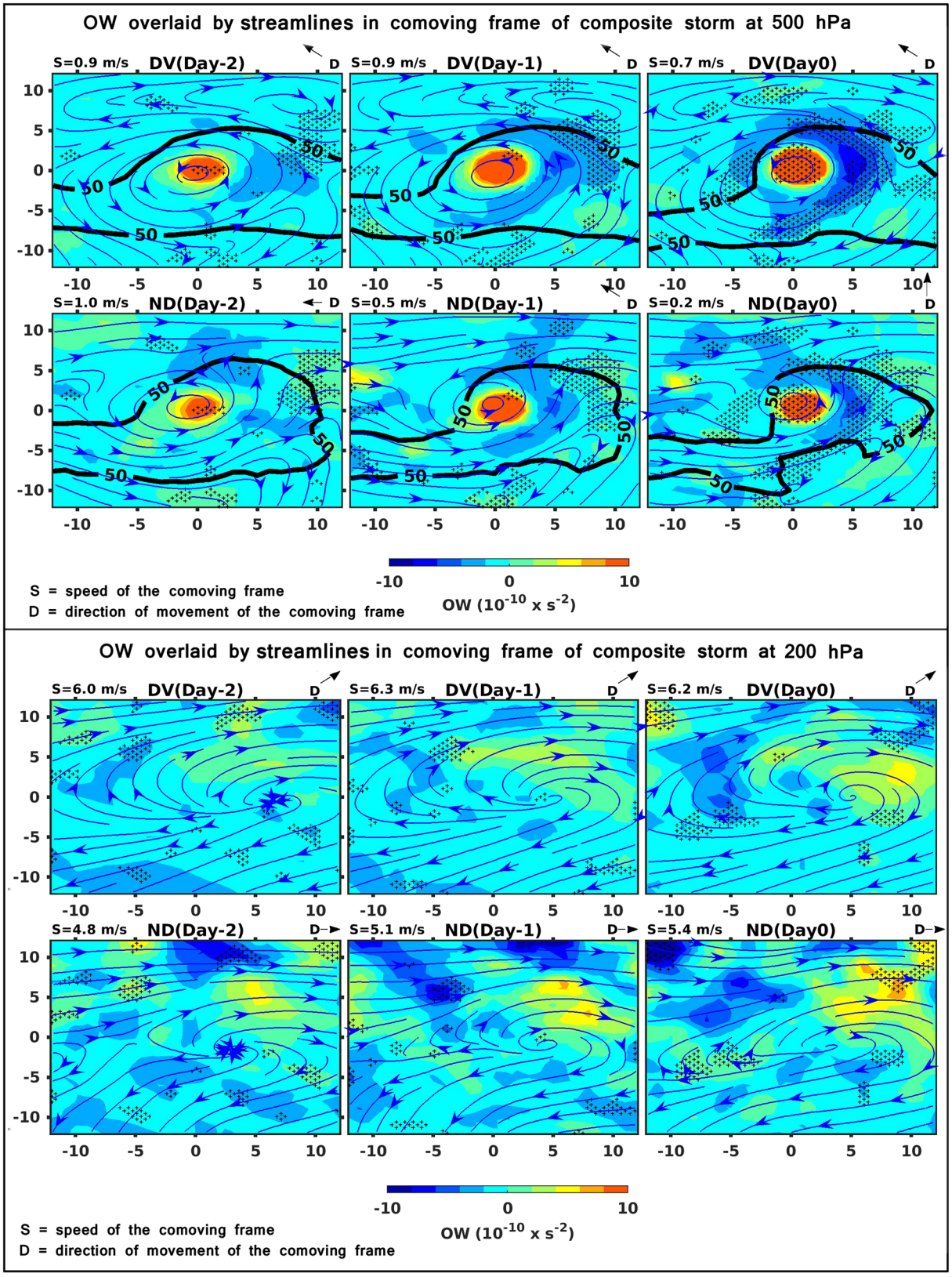

Figure 4. The same as Figure 3 at 500 and 200 hPa; the black contour indicates the 50% RH.

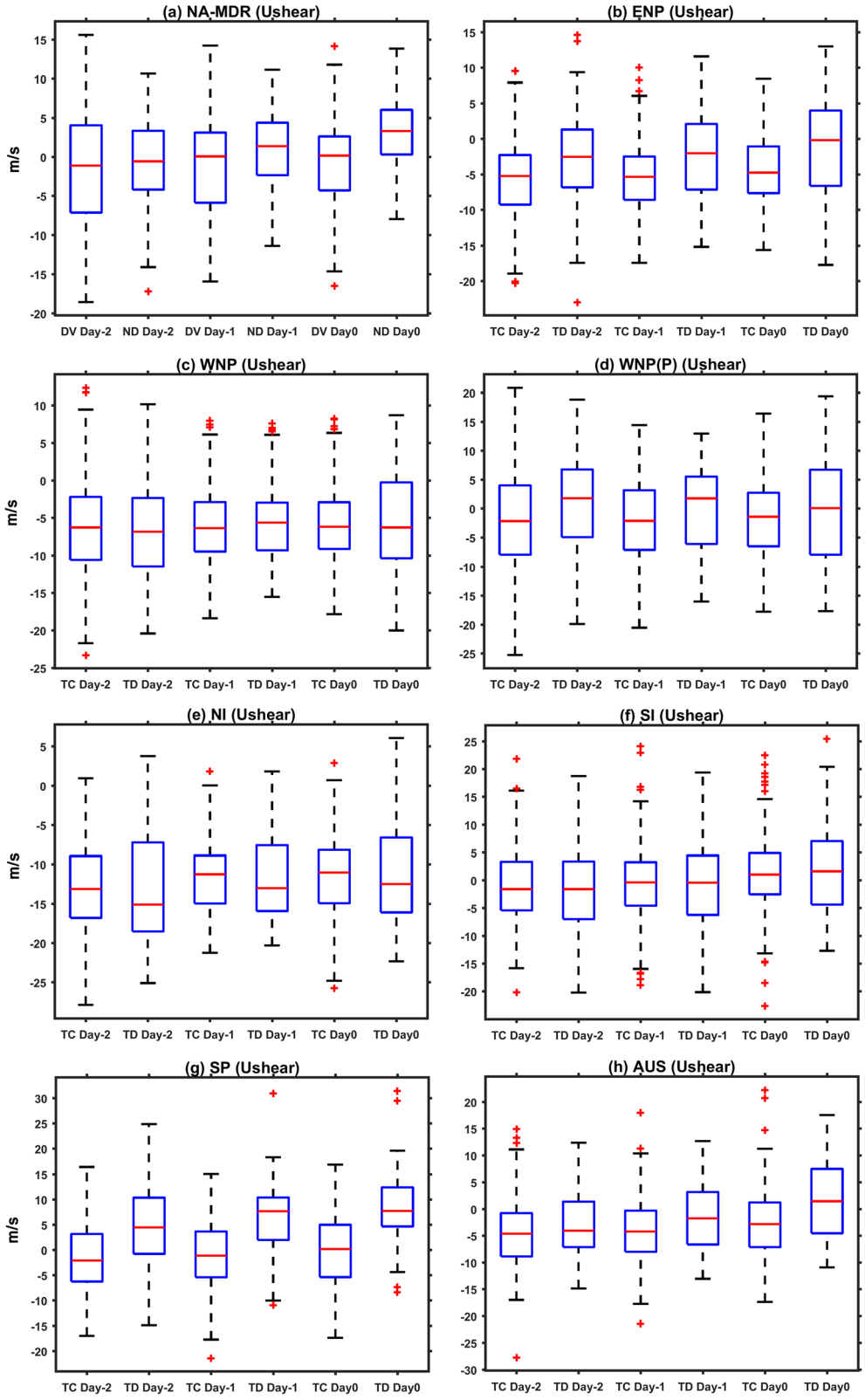

Figure 5. (a–h) Boxplots of averaged Ushear for DV and ND cases within a 12° × 12° box region. The horizontal line of the box indicates median of the distribution, the left and right box edges show 75th and 25th percentiles, the whiskers indicate maximum and minimum values, and the red crosses indicate outliers. The statistical significance of Ushear is given in Figure 6.

As the depression develops, a stronger shear sheath layer forms in the north, east, and west sides of the storm center enclosing the core region in the developing cases. This layer offers higher resistance for the surrounding dry air or opposite signed vorticity to penetrate toward the center. In contrast, nondeveloping cases have a weaker shear sheath layer enclosing a smaller area around the vortex center at 700- and 500-hPa levels (Figures 3 and 4), with a weaker layer on the west side of the storm. The nondeveloping cases in Figure 4 show an intrusion of dry air at the 500-hPa level (as indicated by the 50% RH values in black contour) into the vortex core region on Day 0 from the northwest side of the depression may be due to weaker shear sheath layer. Also, Figure 5a shows that there is an increased mean westerly shear in the ND cases as the circulation approaches Day 0. Shu et al. (2014) noted that westerly shear is detrimental to the development of a TC as it draws in cold, dry air from the poleward side of the storm. Brammer and Thorncroft (2015) noted that moisture in the north and northwest side is an important factor for developing storms from AEWs. Therefore, a less protective vortex having a weaker shear sheath layer particularly in the northwest side of the center, westerly shear, and lower atmospheric moisture content leads to the nondevelopment of initial TDs in the NA basin.

A similar spatial composite analysis is performed in other NH basins (ENP, WNP, and WNP_P), as shown in Figures S3–S5. We separate the WNP basin into equatorward WNP (0–15°N) and poleward WNP_P (15–30°N) regions due to different TD failure rates (Tory et al., 2018). These basins also show that ND cases have weaker shear sheath layers leading to dry air intrusion due to weak mean easterly shear (except in WNP) shown in Figures 5b–5d, thereby disrupts the deep convection suppressing the development of initial depression. Also, the box-averaged values of OW center and OW surrounding variables show that DV cases have higher positive-centered core region with a stronger negative surrounding shear sheath (Tables S4 and S5). In the NI basin (Figure S6), the nondeveloping cases have disorganized circular structure of the centered positive OW core region at middle levels of the troposphere with significantly lower magnitude on Day 0 (Table S4). Also, the ND cases across the NI basin have a weaker shear sheath layer at midlevels (500 hPa) on Day 0 but do not indicate the midlevel dry air intrusion into the center due to favorable mean easterly shear (Figure 5e). Therefore, a lack of organized structure of centered circulation in the ND cases leads to the nondevelopment of the circulation across the NI basin.

3.2.2. SH Basins

The spatial composites of the atmospheric variables in the SH indicate a larger spatial extent with a higher magnitude of these variables in DV cases compared to the ND cases (not shown). Figures S7–S9 show the OW composites overlaid with the streamlines over the SI, SP, and AUS basins, respectively. These basins also depict similar structural features as observed in the NH basins with a stronger cyclonic circulation at low levels and anticyclonic at upper levels. The DV cases have significantly higher OW center values and a stronger shear sheath with stronger negative OW surrounding values from the low (850 hPa) to midtroposphere (500 hPa) (Tables S4 and S5). The ND cases have weaker mean easterly shear or increased westerly shear (Figures 5g and 5h) in SP and AUS basins compared to the DV cases. In contrast, the SI basin has similar mean shear for both DV and ND cases (Figure 5f). Across these ocean basins, the nondeveloping cases have a weaker shear sheath layer on the west side of the depression indicating midlevel dry air intrusion (with 55–60% RH values) to the center of the depression impeding the development of TD. Therefore, a less protected vortex having a weaker shear sheath layer with unfavorable shear disrupts the intensification of the initial circulation to a TS.

3.3. Quantification of Differences From Statistical Distributions Using the BDI

We computed the statistical distributions of the environmental variables averaged within a 12° × 12° box region on Day 2, Day 1, and Day 0 to reveal the variables that show significant differences between the DV and ND cases (Figures S10–S13). Although statistical distributions identify the variables showing significant differences between DV and ND cases, they do not give the order of the important variables. The BDI index, which uses the mean and standard deviation of the samples, describes the relative importance of variables in distinguishing DV from ND and is calculated for each large-scale variable on Day 2, Day 1, and Day 0. In particular, this index identifies which quantities/processes are most detrimental to TS formation. Here, we use both Day 2 and Day 0 BDI values to rank the order of prominent variables (Table 1), including their statistically significance, that hinder/favor the intensification of an initial circulation. The BDI values of

Table 1
The Order of Importance of Variables in Each Ocean Basin Based on the Statistically Significant Values at the 95% Significance Level of the BDI Index at Day 2 and Day 0 (the Day of TD Declaration)

BASIN	Order of variables (Day 2)	Order of variables (Day 0)
NA-MDR	TCW, MPI, Omega, RVor	RVor, TCW, Ushear, Omega
ENP	TCW, Ushear, RVor, Omega	TCW, Ushear, Omega, Beta*
WNP	RVor, Omega, MPI, TCW	RVor, Omega, MPI,TCW
WNP-P	RVor, TCW, Ushear, MPI	RVor, TCW, Omega, MPI
NI	—	Omega
SI	TCW, Omega	TCW, Omega, RVor, MPI
SP	Ushear, MPI, TCW, RVor, Beta*	Ushear, MPI, TCW, RVor, Omega
AUS	RVor, TCW, Ushear	RVor, TCW, Ushear, Omega, MPI

700-hPa RH correlate with TCW, and BDI values of Omega correlate with DIV across all the ocean basins; therefore, we include only TCW and Omega in the BDI discussion.

3.3.1. NH Basins

Across the NA basin, Figure 6a shows that as the DV circulation approaches Day 0, we observe increased updrafts (Omega) and low-level vorticity (RVor) suggesting a developing circulation due to availability of sufficient tropospheric moisture (TCW) from Day 2. This higher moisture favors sustained convection by increasing the efficiency of upward mass flux and thereby increases the strength of the circulation. Also, as the circulation approaches Day 0, we observe that DV cases have favorable mean shear compared to the ND cases that have mean westerly shear (Figure 5a). The lower values of moisture and unfavorable shear lead to disruption of deep convection that suppresses the development in ND cases. Also, the BDI values show that DV cases have higher thermodynamical instability measured in terms of MPI. This analysis shows that tropospheric moisture is an important limiting factor across this basin for an initial circulation to develop into a TS. A few studies noted that the Saharan Air Layer acts as a modulating influence for the TC activity across this basin, as it suppresses the convection, entrains dry air to the center of the circulation, and increases vertical wind shear leading to nondevelopment of the circulation (Dunion & Velden, 2004). Other studies noted that preexistence of a dry troposphere or the advection of the dry air by the AEWs, large-scale subsidence, TC-TC interactions or TC interaction with environment creates a dry atmosphere and higher vertical wind shear that disrupts storm formation (Brammer & Thorncroft, 2015; Braun, 2010; Fowler & Galarneau, 2017; Hopsch et al., 2010). Therefore, the availability of sufficient tropospheric moisture around the disturbance with favorable shear supports the development of the incipient circulation.

From the BDI values across the ENP basin (Figure 6b), as the circulation progresses from Day 2 to Day 0, DV cases have increased TCW at the center and surrounding areas of the circulation along with favorable mean easterly shear (Ushear) compared to the ND cases (Figure 5b). The lower BDI values of RVor indicate that both DV and ND cases have similar low-level vorticity. Therefore, the lack of sufficient tropospheric moisture and unfavorable shear suppresses the development of an ND case across the ENP basin. The limiting variables for TS formation identified from this analysis also agree with other studies at different timescales. For instance, at interannual timescales across the ENP basin, Zhao and Raga (2015) noted that midlevel RH acts as a significant contributor to TS formation in inactive years (i.e., years observed with low TC activity) and vertical wind shear is the most important parameter in the active years (high TC activity).

The WNP basin is the most active basin for TC formation across the global ocean basins due to favorable regional environmental conditions. There is a strong monsoon circulation that provides sufficient low-level convergence and higher sea surface temperatures due to the warm pool region favor TC formation. Nevertheless, there exist environmental differences between DV and ND cases due to the prevalence of different synoptic-scale disturbances across the basin (Fu et al., 2012; Li, 2006; Li & Fu, 2006). The higher BDI values from Figures 6c and 6d show that DV cases have stronger vorticity (RVor) and increased updrafts (Omega) compared to the ND cases. These higher values of vorticity in DV cases from Day 2 indicate that the initial circulation originated in a strongly convective region, which favors further intensification by deep convection. Also, the thermodynamic favorability measured in terms of MPI and TCW is higher for DV cases compared to the ND cases across the entire basin. In addition, across the WNP_P basin, DV cases have favorable mean easterly shear (Ushear) compared to the ND cases (Figure 5d). The initial circulation originating in a weakly convective region with a less thermodynamically unstable environment leads to the nondevelopment across the basin. Therefore, the dynamical condition is more important for the development of an initial circulation across the WNP basin (Fu et al., 2012; Lee, 1989a, 1989b; McBride & Zehr, 1981).

Across the NI Ocean, from the BDI values of Figure 6e, we observe that DV cases have stronger updrafts (Omega) on Day 0 compared to the ND cases. A study by Tsuboi and Takemi (2014) noted that Omega acts as a major contributor the changes in the TC frequency during the active phase of the Madden-Julian

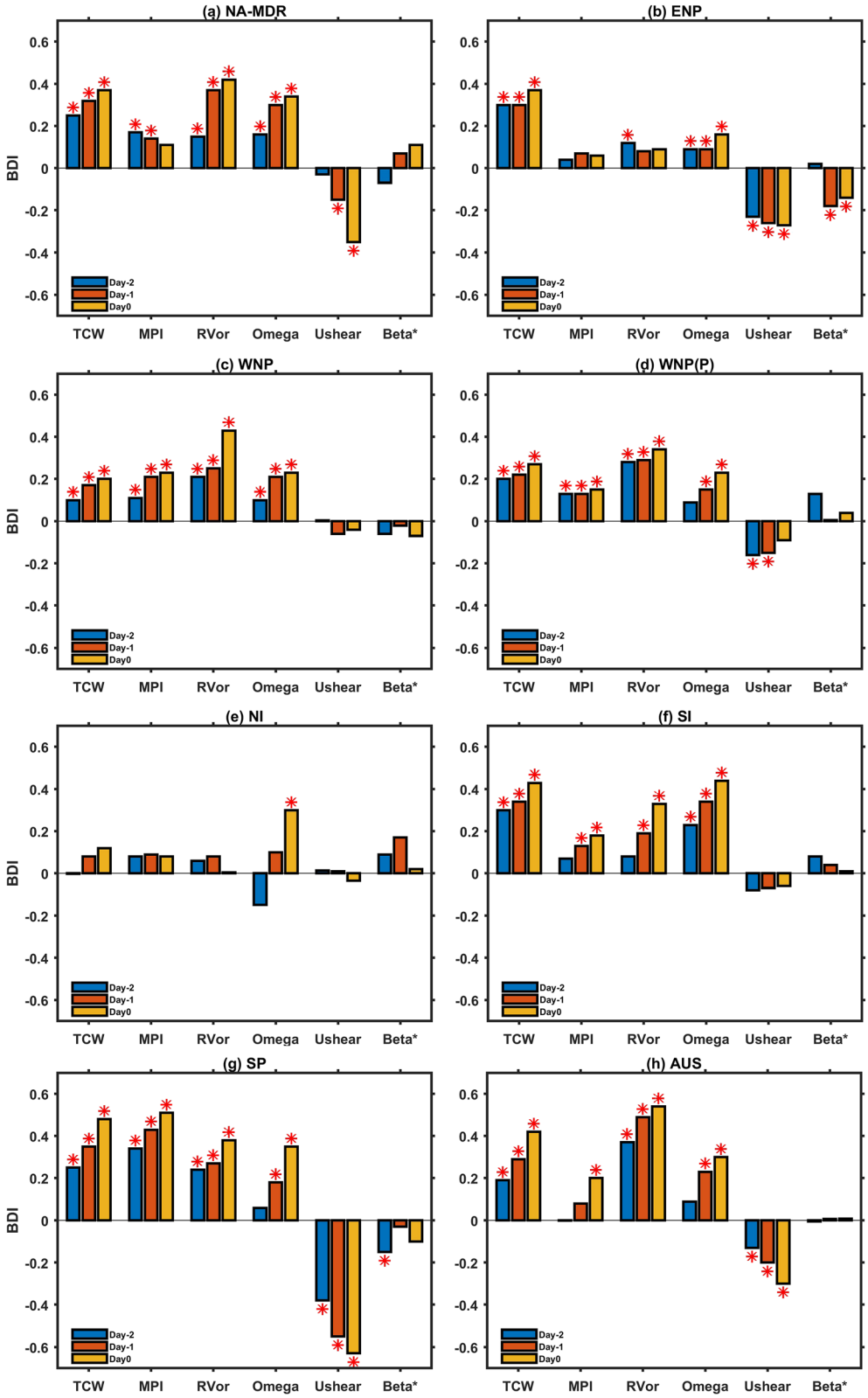

Figure 6. (a–h) Basinwide BDI index of environmental variables for PDV48 and PND48 cases on Day 2, Day 1, and Day 0. Positive values of the BDI index for TCW, MPI, RVor, and Omega indicate more favorable conditions for development, while negative values of Ushear, Beta* are more favorable (* indicates the 95% significance level). For parameterwise comparison of the BDI values refer to Figure S14.

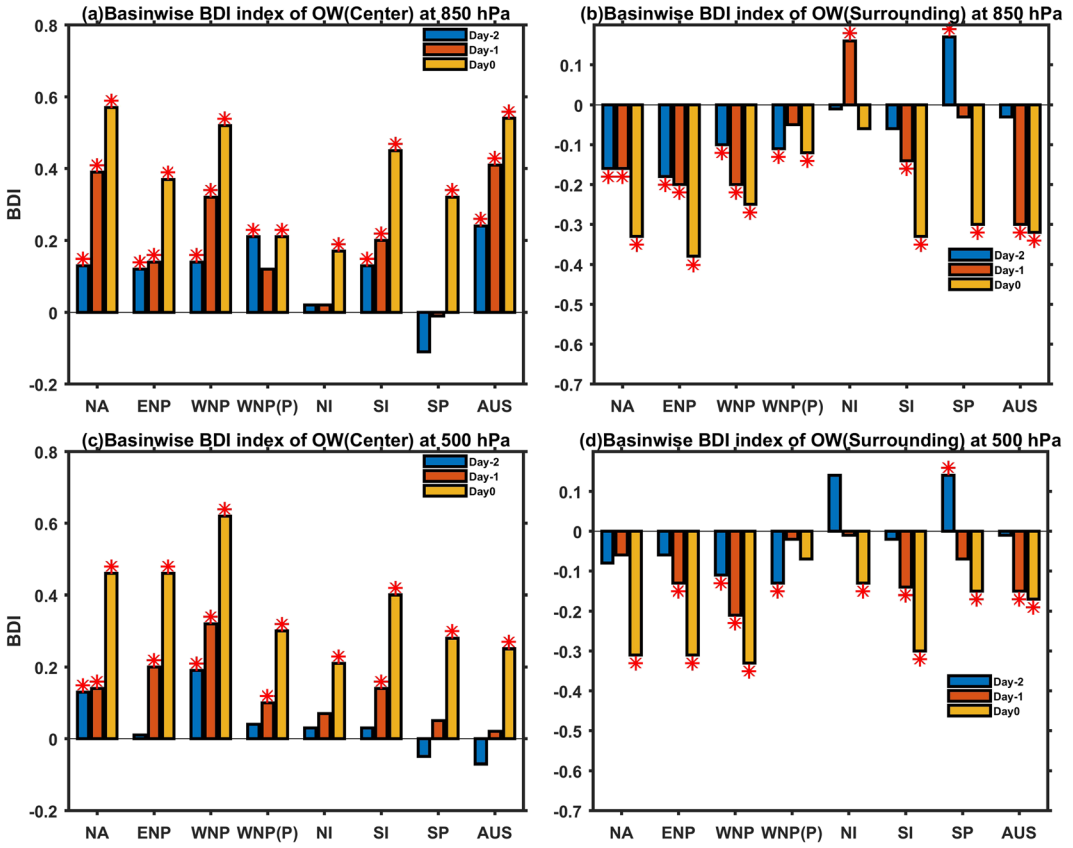

Figure 7. (a–d) Basinwide BDI index of OW center and OW surrounding for DV and ND cases at 850- and 500-hPa levels on Day 2, Day 1, and Day 0. Positive values of OW center variable and negative values of OW surrounding variable are more favorable for TS formation (* indicates a 95% significance level).

Oscillation across this basin. The NI Ocean is a unique basin compared to other basins as it does not observe significant differences for most of the large-scale variables perhaps due to poor performance of TC frequency characteristics using the OWZP scheme (Tory, Chand, Dare, & McBride, 2013).

3.3.2. SH Basins

The BDI analysis over the SH basins shows some similarities with the NH basins in the significant limiting variables with a difference in the order of the variables (Table 1). Figure 6f shows that the DV cases in the SI Ocean have higher TCW, Omega, and RVor compared to the ND cases. Over the SP basin, the BDI values in Figure 6g show that DV cases have favorable thermodynamic conditions and mean easterly shear compared to the ND cases (Figure 5g). Therefore both thermodynamical (MPI and TCW) and dynamical (Ushear) conditions act as the significant influencing variables for the development of a TD across the SP basin. From the BDI values across the AUS basin (Figure 6h), we observe that DV cases have higher RVor and TCW compared to the ND cases. Also, the DV cases have favorable mean easterly shear compared to ND cases (Figure 5h). Earlier studies at different time scales show that sea surface temperatures, vertical wind shear, RH, and RVor are significant influencing variables across SH basins (Camargo et al., 2007; Chand & Walsh, 2011; Dowdy et al., 2012; Kuleshov et al., 2009; Liu & Chan, 2012; Ramsay et al., 2008).

In addition to the above large-scale variables, we estimate the BDI index of the Beta*, OW center, and OW surrounding variables across these ocean basins. The Beta* variable, which shows the barotropic instability regions, is found to differentiate the DV and ND cases across the ENP and SP basins. Also, from the BDI index values of the OW center variable (Figure 7), we observe that developing cases have higher magnitudes of OW center across all the ocean basins, indicating strong low-deformation vorticity regions. Also, the BDI values of the OW surrounding variable (Figure 7) show that DV cases have stronger negative values compared to the ND cases in most of the ocean basins, indicating a stronger shear sheath that protects the vortex from external negative influences. Therefore, in addition to the above large-scale variables, the Beta*,

OW center, and OW surrounding parameters can be used as predictors across the ocean basins to discriminate the DV and ND cases.

4. Discussion

The circulation-centered spatial composites of the RH, DIV, and MPI variables evolving from Day 2 to Day 0 show that developing cases have more considerable spatial extent surrounding the vortex core of a region of the higher magnitude of these variables (Figure 2). In contrast, the nondeveloping cases have less spatial extent and lower values of the environmental conditions from Day 2. The Ushear spatial composites show that nondeveloping cases have either strong mean westerly shear or weak easterly shear unfavorable for TS formation. The composites of the streamlines overlaid with shaded OW parameter and RH contours help us to identify the structural variations between DV and ND cases (Figures 3 and 4). These composites show that nondeveloping cases have lower values of centered OW along with a weaker band of negative OW values (the shear sheath) surrounding the core region from lower levels to midlevels compared to the DV cases across most of the basins (Tables S4 and S5). In contrast, developing cases have stronger OW core regions and a stronger surrounding shear sheath layer from lower levels to midlevels. Also, DV cases have mean easterly wind shear, which draws the warm moist air from the equatorward side of the storm (Shu et al., 2014). In ND cases, the increased westerly shear or weak easterly shear, as well as a weaker shear sheath in the west or northwest side of the vortex center on Day 0, may lead to horizontal entrainment of surrounding drier air at midtroposphere (500 hPa) in some of the basins. Drawing the cold, dry air from the side with a weaker shear sheath layer may disrupt the storm formation in ND cases by reducing the overall moisture content and affecting the sustained convection. In contrast to the above results, across the NI basin, both DV and ND cases have easterly shear and weaker shear sheath region. However, an unorganized structure of the OW-centered values leads to the nondevelopment of the initial circulation in this basin. Therefore, a more compact vertical structure from lower levels to midlevels with a stronger centered vortex along with a stronger shear sheath layer protects the incipient circulation.

The BDI index illustrates the relative importance of the thermodynamical and dynamical conditions on the development of TS from an initial circulation. The BDI magnitude (Figures 6 and S14) from Day 2 to Day 0 shows that environmental differences between DV and ND gradually increase from Day 2 to Day 0. These differences indicate that either DV cases are in favorable environmental conditions or there is the increased influence of destructive forces in ND cases. Table 1, which shows the order of important variables, notes slight differences in the order of these influencing variables on Day 2 and Day 0, with similar environmental variables appearing to be prominent on both days but with a larger magnitude on Day 0. Figure 6 gives an overview of the role of environmental variables on the development of an initial circulation from the BDI values. It shows some agreement between the global ocean basins. For instance, TCW, RVor, and Omega variables show significant differences between DV and ND cases with a higher magnitude of BDI index in almost all the ocean basins. In contrast, MPI, Ushear, and Beta* show differences and seem to play a role in fewer ocean basins.

Although the current analysis does not illustrate the precise convective processes leading to the development of a TS, Figure 6 shows that the DV cases have higher moisture over different ocean basins indicated by positive BDI values of TCW. The higher tropospheric moisture favors sustained deep convection that leads to a strong low-level to midlevel vorticity concentration due to increased convective heating (Z. Wang, 2014; Z. Wang et al., 2012). In contrast, the ND cases that have a drier troposphere lead to weaker deep convection due to weaker updrafts and downdrafts (James & Markowski, 2009; Kilroy & Smith, 2013). Some earlier studies noted that the thermodynamical variable MPI is a vital predictor to determine the TS formation using statistically derived genesis potential indices (Bruyère et al., 2012; Emanuel & Nolan, 2004). This MPI acts as one of the significant influencing factors across the WNP, WNP_P, NA, SP, and AUS basins indicating favorable thermodynamic instability in developing cases.

In the examination of the dynamical variables, Figure 6 shows that the ND cases have lower values of RVor and Omega across all the ocean basins except over the ENP and the NI (Figure 6). The higher magnitudes of RVor and Omega indicate sustained convection and abundant low-level convergence, favorable for TS formation (Montgomery & Smith, 2010; Tory & Frank, 2010). Also, ND cases have weaker mean easterly shear or increased westerly shear across the ocean basins except in the WNP (0–15°N), NI, and the SI basins

(Figure 5), indicating that weak mean easterly shear or increased westerly shear may be detrimental to TS formation. Ritchie and Frank (2007) showed that easterly shear could offset the northwesterly shear induced by the vortex due to the beta effect as the possible reason for westerly shear being detrimental to development. In contrast to the above differences, there are no significant environmental differences between DV and ND cases across the NI basin except for Omega. The BDI analysis shows some similarities between the ocean basins with similar prominent variables. However, the order of these variables varies from basin to basin, perhaps due to distinct large-scale disturbances, different modulating influences, and differences in the background environmental conditions. Also, DV cases have higher positive BDI values of OW center variable and higher negative BDI values of OW surrounding variable favorable for TS formation in most of the basins (Figure 7). Therefore, observing the OW values at the center and surrounding the circulation center from low troposphere to midtroposphere in numerical weather prediction models or including the OW center and OW surrounding variables in statistical models may improve the forecast accuracy of the TS formation from a depression stage vortex.

5. Conclusion

The differences in the large-scale disturbances and the mean flow conditions across the global ocean basins may lead to differences in the relative contribution of large-scale variables to TS formation. Therefore, in this study, we perform a basinwide statistical analysis on the environmental differences between developing and nondeveloping depressions by following the depression two days before its declaration in a Lagrangian manner. We use a previously developed TC detection technique to detect both developing and nondeveloping tropical circulations in the ERA-Interim reanalysis. The spatial composites of atmospheric variables and streamlines from Day 2 to Day 0 help us to monitor the evolving flow features around the depression in each ocean basin. We employ a statistical BDI index to quantitatively identify the order of important atmospheric variables that distinguish the developing and nondeveloping depressions across each ocean basin. We find the following main conclusions:

1. The spatial composites of the environmental variables show that DV cases have more favorable conditions at the center and surrounding compared to the nondeveloping cases from 2 days before TD declaration (Figure 2).
2. The DV cases have a protective vortex with a strong positive OW core region and the development of a surrounding region of stronger negative OW, the “shear sheath,” from the low troposphere to midtroposphere as it approaches TD declaration stage (Day 0). In contrast, nondeveloping cases have less protective vortex with a weaker shear sheath in the northwest/west side of the depression, leading to the intrusion of cold, dry air to the center of the circulation at midlevels (500 hPa) on Day 0 (Figures 3 and 4).
3. The ND cases have either mean westerly shear or weaker mean easterly shear in some ocean basins (Figure 5), which leads to dry air intrusion disrupting the intensification of the vortex.
4. Based on the BDI values on Day 2 and Day 0 (Table 1), TCW and RVor act as significant limiting factors for TS formation over the NA; RVOR over the WNP basins; TCW, and Ushear over the ENP basin; and Omega over the NI basin. In SH, TCW, and Omega act as main limiting factors for TS formation over the SI; Ushear, and MPI over the SP; and RVor and TCW over the AUS basin. This BDI analysis shows that TCW and RVor are important in most of the ocean basins and Ushear, which shows that the large-scale influence is prominent in a few ocean basins (Figure 6).
5. The BDI values of the OW center and OW surrounding variables show that DV cases have stronger core and stronger shear sheath from Day 2 compared to the ND cases in most of the ocean basins (Figure 7).

This study provides a set of large-scale environmental conditions that act as limiting factors for the development of an initial TD to TS across each ocean basin. We observe similar structural differences between developing and nondeveloping TDs across most of the ocean basins. In contrast, there are varying contributions of environmental variables that may be due to the distinct large-scale disturbances and their interactions with the basin's mean flow conditions. This study identifies additional predictors for the TS formation forecast in addition to earlier large-scale variables. Therefore, the inclusion of both OW center and OW surrounding variables in building statistical forecast models of TS formation from the initial depressions along with other atmospheric variables such as TCW, MPI, RVor, Omega, Ushear may improve TS forecasts at the synoptic scale. Future work focuses on the application of this methodology to forecast

analysis fields to observe whether similar large-scale variables act as impediments for the TS formation from an initial circulation and establish a statistical TS formation forecast model. Also, more detailed analysis will be necessary to understand the variations in the order of important variables across the global ocean basins, which improves our understanding of the relationship between large-scale environmental variables and TS formation.

Acknowledgments

We acknowledge valuable discussions with Kevin Tory and the constructive comments of three anonymous reviewers. We are grateful to the financial support for the Ph.D. from the Melbourne India Postgraduate Program. We thank the National Computational Infrastructure System, supported by the Australian Government, for providing the preprocessed ERA-Interim data and computational resources. The authors are thankful for the Australian Research Council Centre of Excellence for Climate Extremes and Earth Systems and Climate Change Hub of the National Environmental Science Program for supplying partial financial support. The ERA-Interim reanalysis data used for current analysis is available at the following link (https://apps.ecmwf.int/datasets/data/interim-full-daily/levtype=pl/).

References

Alland, J. J., Tang, B. H., & Corbosiero, K. L. (2017). Effects of midlevel dry air on development of the axisymmetric tropical cyclone secondary circulation. *Journal of the Atmospheric Sciences*, *74*(5), 1455–1470.

Asaadi, A., Brunet, G., & Yau, M. K. (2016). On the dynamics of the formation of the Kelvin cat's-eye in tropical cyclogenesis. Part I: Climatological investigation. *Journal of the Atmospheric Sciences*, *73*(6), 2317–2338.

Asaadi, A., Brunet, G., & Yau, M. K. (2017). The importance of critical layer in differentiating developing from nondeveloping easterly waves. *Journal of the Atmospheric Sciences*, *74*(2), 409–417.

Avila, L. A. (1991). Atlantic tropical systems of 1990. *Monthly Weather Review*, *119*(8), 2027–2033.

Bell, S. S., Chand, S. S., Tory, K. J., & Turville, C. (2018). Statistical assessment of the OWZ tropical cyclone tracking scheme in ERA-Interim. *Journal of Climate*, *31*, 2217–2232.

Bessafi, M., & Wheeler, M. C. (2006). Modulation of South Indian Ocean tropical cyclones by the Madden–Julian oscillation and convectively coupled equatorial waves. *Monthly Weather Review*, *134*(2), 638–656.

Bister, M., & Emanuel, K. A. (1998). Dissipative heating and hurricane intensity. *Meteorology and Atmospheric Physics*, *50*, 233–240.

Brammer, A., & Thorncroft, C. D. (2015). Variability and evolution of African easterly wave structures and their relationship with tropical cyclogenesis over the eastern Atlantic. *Monthly Weather Review*, *143*(12), 4975–4995.

Braun, S. A. (2010). Reevaluating the role of the Saharan air layer in Atlantic tropical cyclogenesis and evolution. *Monthly Weather Review*, *138*(6), 2007–2037.

Briegel, L. M., & Frank, W. M. (1997). Large-scale influences on tropical cyclogenesis in the western North Pacific. *Monthly Weather Review*, *125*(7), 1397–1413.

Bruyère, C. L., Holland, G. J., & Towler, E. (2012). Investigating the use of a genesis potential index for tropical cyclones in the North Atlantic basin. *Journal of Climate*, *25*(24), 8611–8626.

Camargo, S. J., Emanuel, K. A., & Sobel, A. H. (2007). Use of a genesis potential index to diagnose ENSO effects on tropical cyclone genesis. *Journal of Climate*, *20*(19), 4819–4834.

Chand, S. S., & Walsh, K. J. (2011). Forecasting tropical cyclone formation in the Fiji region: A probit regression approach using a Bayesian fitting. *Weather and Forecasting*, *26*(2), 150–165.

Compo, G. P., Whitaker, J. S., Sardeshmukh, P. D., Matsui, N., Allan, R. J., Yin, X., et al. (2011). The twentieth century reanalysis project. *Quarterly Journal of the Royal Meteorological Society*, *137*(654), 1–28.

Davis, C. A., & Ahijevych, D. A. (2012). Mesoscale structural evolution of three tropical weather systems observed during PREDICT. *Journal of the Atmospheric Sciences*, *69*(4), 1284–1305.

Dee, D. P., Uppala, S. M., Simmons, A. J., Berrisford, P., Poli, P., Kobayashi, S., et al. (2011). The ERA-Interim reanalysis: Configuration and performance of the data assimilation system. *Quarterly Journal of the Royal Meteorological Society*, *137*(656), 553–597.

Ditchek, S. D., Nelson, T. C., Rosenmayer, M., & Corbosiero, K. L. (2017). The relationship between tropical cyclones at genesis and their maximum attained intensity. *Journal of Climate*, *30*(13), 4897–4913.

Dowdy, A. J., Qi, L., Jones, D., Ramsay, H., Fawcett, R., & Kuleshov, Y. (2012). Tropical cyclone climatology of the South Pacific Ocean and its relationship to El Niño–Southern Oscillation. *Journal of Climate*, *25*(18), 6108–6122.

Dunion, J. P., & Velden, C. S. (2004). The impact of the Saharan air layer on Atlantic tropical cyclone activity. *Bulletin of the American Meteorological Society*, *85*(3), 353–365.

Dunkerton, T. J., Montgomery, M. T., & Wang, Z. (2009). Tropical cyclogenesis in a tropical wave critical layer: Easterly waves. *Atmospheric Chemistry and Physics*, *9*(15).

Emanuel, K. & Nolan, D. S. (2004). Tropical cyclone activity and the global climate system. Extended Abstracts, 26th Conf. on Hurricanes and Tropical Meteorology, Miami, FL, Amer. Meteor. Soc., 240–241.

Ferreira, R. N., & Schubert, W. H. (1997). Barotropic aspects of ITCZ breakdown. *Journal of the Atmospheric Sciences*, *54*(2), 261–285.

Fowler, J. P., & Galarneau, T. J. Jr. (2017). Influence of storm–storm and storm–environment interactions on tropical cyclone formation and evolution. *Monthly Weather Review*, *145*(12), 855–4875.

Frank, W. M., & Roundy, P. E. (2006). The role of tropical waves in tropical cyclogenesis. *Monthly Weather Review*, *134*(9), 2397–2417.

Fu, B., Li, T., Peng, M. S., & Weng, F. (2007). Analysis of tropical cyclogenesis in the western North Pacific for 2000 and 2001. *Weather and Forecasting*, *22*(4), 763–780.

Fu, B., Peng, M. S., Li, T., & Stevens, D. E. (2012). Developing versus nondeveloping disturbances for tropical cyclone formation. Part II: Western North Pacific. *Monthly Weather Review*, *140*(4), 1067–1080.

Gray, W. M. (1968). Global view of the origin of tropical disturbances and storms. *Monthly Weather Review*, *110*, 548–586.

Gray, W. M. (1975). Tropical cyclone genesis. *Atmospheric Sciences*, (pp. 234).

Hall, J. D., Matthews, A. J., & Karoly, D. J. (2001). The modulation of tropical cyclone activity in the Australian region by the Madden–Julian oscillation. *Monthly Weather Review*, *129*(12), 2970–2982.

Hendricks, E. A., Montgomery, M. T., & Davis, C. A. (2004). The role of "vortical" hot towers in the formation of tropical cyclone Diana (1984). *Journal of the Atmospheric Sciences*, *61*(11), 1209–1232.

Hopsch, S. B., Thorncroft, C. D., & Tyle, K. R. (2010). Analysis of African easterly wave structures and their role in influencing tropical cyclogenesis. *Monthly Weather Review*, *138*(4), 1399–1419.

James, R. P., & Markowski, P. M. (2009). A numerical investigation of the effects of dry air aloft on deep convection. *Mon. Weather Rev*, *138*, 140–161.

Kilroy, G., & Smith, R. K. (2013). A numerical study of rotating convection during tropical cyclogenesis. *Quarterly Journal of the Royal Meteorological Society*, *139*, 1255–1269.

Knapp, K. R., Kruk, M. C., Levinson, D. H., Diamond, H. J., & Neumann, C. J. (2010). The international best track archive for climate stewardship (IBTrACS) unifying tropical cyclone data. *Bulletin of the American Meteorological Society*, *91*(3), 363–376.

Komaromi, W. A. (2013). An investigation of composite dropsonde profiles for developing and nondeveloping tropical waves during the 2010 PREDICT field campaign. *Journal of the Atmospheric Sciences*, *70*(2), 542–558.
Kuleshov, Y., Chane-Ming, F., Qi, L., Chouaibou, I., Hoareau, C., & Roux, F. (2009). Tropical cyclone genesis in the Southern Hemisphere and its relationship with the ENSO. *Annales Geophysicae*, *27*(6), 2523–2538.
Landsea, C. W. (1993). A climatology of intense (or major) Atlantic hurricanes. *Monthly Weather Review*, *121*, 1703–1712.
Lee, C. S. (1989a). Observational analysis of tropical cyclogenesis in the western North Pacific. Part I: Structural evolution of cloud clusters. *Journal of the Atmospheric Sciences*, *46*(16), 2580–2598.
Lee, C. S. (1989b). Observational analysis of tropical cyclogenesis in the western North Pacific. Part II: Budget analysis. *Journal of the Atmospheric Sciences*, *46*(16), 2599–2616.
Lee, C. S., Edson, R., & Gray, W. M. (1989). Some large-scale characteristics associated with tropical cyclone development in the North Indian Ocean during FGGE. *Monthly Weather Review*, *117*(2), 407–426.
Li, T. (2006). Origin of the summertime synoptic-scale wave train in the western North Pacific. *Journal of the Atmospheric Sciences*, *63*(3), 1093–1102.
Li, T., & Fu, B. (2006). Tropical cyclogenesis associated with Rossby wave energy dispersion of a preexisting typhoon. Part I: Satellite data analyses. *Journal of the Atmospheric Sciences*, *63*(5), 1377–1389.
Li, T., Ge, X., Wang, B., & Zhu, Y. (2006). Tropical cyclogenesis associated with Rossby wave energy dispersion of a preexisting typhoon. Part II: Numerical simulations. *Journal of the Atmospheric Sciences*, *63*(5), 1390–1409.
Liu, K. S., & Chan, J. C. (2012). Interannual variation of Southern Hemisphere tropical cyclone activity and seasonal forecast of tropical cyclone number in the Australian region. *International Journal of Climatology*, *32*(2), 190–202.
McBride, J. L., & Zehr, R. (1981). Observational analysis of tropical cyclone formation. Part II: Comparison of non-developing versus developing systems. *Journal of the Atmospheric Sciences*, *38*(6), 1132–1151.
Montgomery, M. T., Lussier III, L. L., Moore, R. W., & Wang, Z. (2010). The genesis of Typhoon Nuri as observed during the tropical cyclone structure 2008 (TCS-08) field experiment—Part 1: The role of the easterly wave critical layer. *Atmospheric Chemistry and Physics*, *10*(20), 9879–9900.
Montgomery, M. T., Nicholls, M. E., Cram, T. A., & Saunders, A. B. (2006). A vortical hot tower route to tropical cyclogenesis. *Journal of the Atmospheric Sciences*, *63*(1), 355–386.
Montgomery, M. T. & Smith, R. K. (2010). Tropical-cyclone formation: Theory and idealized modelling. Naval postgraduate school Monterey CA, Dept. Meteorol.
Nolan, D. S. (2007). What is the trigger for tropical cyclogenesis? *Australian Meteorological Magazine*, *56*, 241–266.
Peng, M. S., Fu, B., Li, T., & Stevens, D. E. (2012). Developing versus nondeveloping disturbances for tropical cyclone formation. Part I: North Atlantic. *Monthly Weather Review*, *140*(4), 1047–1066.
Ramsay, H. A., Leslie, L. M., Lamb, P. J., Richman, M. B., & Leplastrier, M. (2008). Interannual variability of tropical cyclones in the Australian region: Role of large-scale environment. *Journal of Climate*, *21*(5), 1083–1103.
Raymond, D. J., & Sessions, S. L. (2007). Evolution of convection during tropical cyclogenesis. *Geophysical Research Letters*, *34*, L06811. https://doi.org/10.1029/2006GL028607
Riemer, M., Montgomery, M. T., & Nicholls, M. E. (2010). A new paradigm for intensity modification of tropical cyclones: Thermodynamic impact of vertical wind shear on the inflow layer. *Atmospheric Chemistry and Physics*, *10*(7).
Ritchie, E. A., & Frank, W. M. (2007). Interactions between simulated tropical cyclones and an environment with a variable Coriolis parameter. *Monthly Weather Review*, *135*(5), 1889–1905.
Ritchie, E. A., & Holland, G. J. (1999). Large-scale patterns associated with tropical cyclogenesis in the western Pacific. *Monthly Weather Review*, *127*(9), 2027–2043.
Rozoff, C. M., Schubert, W. H., McNoldy, B. D., & Kossin, J. P. (2006). Rapid filamentation zones in intense tropical cyclones. *Journal of the Atmospheric Sciences*, *63*(1), 325–340.
Rutherford, B., Boothe, M. A., Dunkerton, T. J., & Montgomery, M. T. (2018). Dynamical properties of developing tropical cyclones using Lagrangian flow topology. *Quarterly Journal of the Royal Meteorological Society*, *144*(710), 218–230.
Rutherford, B., Dunkerton, T. J., & Montgomery, M. T. (2015). Lagrangian vortices in developing tropical cyclones. *Quarterly Journal of the Royal Meteorological Society*, *141*(693), 3344–3354.
Sears, J., & Velden, C. S. (2014). Investigating the role of the upper-levels in tropical cyclone genesis. *Tropical Cyclone Research and Review*, *3*(2), 91–110.
Shu, S., Zhang, F., Ming, J., & Wang, Y. (2014). Environmental influences on the intensity changes of tropical cyclones over the western North Pacific. *Atmospheric Chemistry and Physics*, *14*(12), 6329–6342.
Smith, R. K., & Montgomery, M. T. (2012). Observations of the convective environment in developing and non-developing tropical disturbances. *Quarterly Journal of the Royal Meteorological Society*, *138*(668), 1481–1739.
Tang, B., & Emanuel, K. (2010). Midlevel ventilation's constraint on tropical cyclone intensity. *Journal of the Atmospheric Sciences*, *67*(6), 1817–1830.
Thorncroft, C. D., & Hodges, K. (2001). African easterly wave variability and its relationship to Atlantic tropical cyclone activity. *Journal of Climate*, *14*, 1166–1179.
Tippett, M. K., Camargo, S. J., & Sobel, A. H. (2011). A Poisson regression index for tropical cyclone genesis and the role of large-scale vorticity in genesis. *Journal of Climate*, *24*(9), 2335–2357.
Tory, K. J., Chand, S. S., Dare, R. A., & McBride, J. L. (2013). The development and assessment of a model-, grid-, and basin-independent tropical cyclone detection scheme. *Journal of Climate*, *26*(15), 5493–5507.
Tory, K. J., Chand, S. S., McBride, J. L., Ye, H., & Dare, R. A. (2013). Projected changes in late-twenty-first-century tropical cyclone frequency in 13 coupled climate models from phase 5 of the Coupled Model Intercomparison Project. *Journal of Climate*, *26*(24), 9946–9959.
Tory, K. J., Dare, R. A., Davidson, N. E., McBride, J. L., & Chand, S. S. (2013). The importance of low-deformation vorticity in tropical cyclone formation. *Atmospheric Chemistry and Physics*, *13*(4), 2115–2132.
Tory, K. J., Davidson, N. E., & Montgomery, M. T. (2007). Prediction and diagnosis of tropical cyclone formation in an NWP system. Part III: Diagnosis of developing and nondeveloping storms. *Journal of the Atmospheric Sciences*, *64*(9), 3195–3213.
Tory K. J., & Frank, W. M. (2010). Tropical cyclone formation. Chapter 2: Global perspectives on tropical cyclones. In: Chan J, Kepert JD (eds) world scientific, Second Edition.
Tory, K. J., Montgomery, M. T., & Davidson, N. E. (2006). Prediction and diagnosis of tropical cyclone formation in an NWP system. Part I: The critical role of vortex enhancement in deep convection. *Journal of the Atmospheric Sciences*, *63*(12), 3077–3090.

Tory, K. J., Montgomery, M. T., Davidson, N. E., & Kepert, J. D. (2006). Prediction and diagnosis of tropical cyclone formation in an NWP system. Part II: A diagnosis of tropical cyclone Chris formation. *Journal of the Atmospheric Sciences*, *63*(12), 3091–3113.

Tory, K. J., Ye, H., & Dare, R. A. (2018). Understanding the geographic distribution of tropical cyclone formation for applications in climate models. *Climate Dynamics*, *50*(7–8), 2489–2512.

Tsuboi, A., & Takemi, T. (2014). The interannual relationship between MJO activity and tropical cyclone genesis in the Indian Ocean. *Geoscience Letters*, *1*(1), 9.

Tuleya, R. E. (1991). Sensitivity studies of tropical storm genesis using a numerical model. *Monthly Weather Review*, *119*(3), 481–733.

Tuleya, R. E., & Kurihara, Y. (1981). A numerical study on the effects of environmental flow on tropical storm genesis. *Monthly Weather Review*, *109*(12), 2487–2506.

Tuleya, R. E., & Kurihara, Y. (1982). A note on the sea surface temperature sensitivity of a numerical model of tropical storm genesis. *Monthly Weather Review*, *110*(12), 2063–2069.

Wang, C. C., & Magnusdottir, G. (2005). ITCZ breakdown in three-dimensional flows. *Journal of the Atmospheric Sciences*, *62*(5), 1497–1512.

Wang, C. C., & Magnusdottir, G. (2006). The ITCZ in the central and eastern Pacific on synoptic time scales. *Monthly Weather Review*, *134*(5), 1405–1421.

Wang, Z. (2012). Thermodynamic aspects of tropical cyclone formation. *Journal of the Atmospheric Sciences*, *69*(8), 2433–2451.

Wang, Z. (2014). Role of cumulus congestus in tropical cyclone formation in a high-resolution numerical model simulation. *Journal of the Atmospheric Sciences*, *71*(5), 1681–1700.

Wang, Z., Montgomery, M. T., & Dunkerton, T. J. (2010a). Genesis of pre–Hurricane Felix (2007). Part I: The role of the easterly wave critical layer. *Journal of the Atmospheric Sciences*, *67*(6), 1711–1489.

Wang, Z., Montgomery, M. T., & Dunkerton, T. J. (2010b). Genesis of pre–Hurricane Felix (2007). Part II: Warm core formation, precipitation evolution, and predictability. *Journal of the Atmospheric Sciences*, *67*(6), 1730–1744.

Wang, Z., Montgomery, M. T., & Fritz, C. (2012). A first look at the structure of the wave pouch during the 2009 PREDICT–GRIP dry runs over the Atlantic. *Monthly Weather Review*, *140*(4), 1144–1163.

Xu, Y., Li, T., & Peng, M. (2013). Tropical cyclogenesis in the western North Pacific as revealed by the 2008–09 YOTC data. *Weather and Forecasting*, *28*(4), 1038–1056.

Zehr, R. (1992). Tropical cyclogenesis in the western North Pacific. NOAA Tech. Rep. 61, 181pp.

Zeng, Z., Wang, Y., & Chen, L. (2010). A statistical analysis of vertical shear effect on tropical cyclone intensity change in the North Atlantic. *Geophysical Research Letters*, *37*, L02802. https://doi.org/10.1029/2009GL041788

Zhang, D. L., & Zhu, L. (2012). Roles of upper-level processes in tropical cyclogenesis. *Geophysical Research Letters*, *39*, L17804. https://doi.org/10.1029/2012GL053140

Zhao, H., & Raga, G. B. (2015). On the distinct interannual variability of tropical cyclone activity over the eastern North Pacific. *Atmosfera*, *28*, 161–178.

Zong, H., & Wu, L. (2015). Re-examination of tropical cyclone formation in monsoon troughs over the western North Pacific. *Advances in Atmospheric Sciences*, *32*(7), 924–934.